Journal of Organometallic Chemistry, 394 (1990) 455–468
Elsevier Sequoia S.A., Lausanne
JOM 20728

The syntheses, structures and stereodynamics of transition metal complexes of 1,1′-bis(methylthio)ruthenocene. Crystal structure of 1,1′-bis(methylthio)ruthenocene tetracarbonyltungsten *

Edward W. Abel, Nicholas J. Long, Keith G. Orrell, Anthony G. Osborne, Vladimír Šik

Department of Chemistry, University of Exeter, Devon. EX4 4QD (U.K.)

Paul A. Bates and Michael B. Hursthouse

Department of Chemistry, Queen Mary College, London E1 4NS (U.K.)

(Received January 4th, 1990)

Abstract

The complexes *cis*-[$M(CO)_4(L–L)$], *fac*-[$ReX(CO)_3(L–L)$] and *fac*-[$PtXMe_3(L–L)$], (M = Cr, Mo, W; L–L = [$(C_5H_4SCH_3)_2Ru$]; X = Cl, Br, I) have been synthesised. A ^1H NMR study of their solution properties has shown that pyramidal inversion of the coordinated sulphur atoms is rapid on the NMR timescale at ambient temperature. At low temperatures (ca. −90 °C) the motion is arrested and the tungsten complex exists as a mixture of *meso* and DL species in approximately equal proportions, whereas the rhenium complexes are predominantly (⩾ 94%) in the *meso* form. Insolubility precluded low-temperature studies on the platinum complexes. Variable temperature bandshape analyses of the tungsten complex yielded a sulphur inversion (*meso* → DL) value of $\Delta G^{\ddagger}$ (298 K) 32.0 ± 1.0 kJ mol^{-1}. The massive predominance of one invertomer in the case of the rhenium complexes prevented a study of the sulphur inversion by bandshape analysis. The crystal structure of 1,1′-bis(methylthio)ruthenocene tetracarbonyltungsten has been determined. The W–S bond lengths are 2.571(5) and 2.565(4) Å, with a S–W–S bond angle of 81.1(1)°. The cyclopentadienyl rings are eclipsed and the S–CH_3 groups adopt a *meso* relationship.

---

* Dedicated to Professor F.G.A. Stone on the occasion of his 65th birthday.

0022-328X/90/$03.50

Introduction

In continuation of our dynamic NMR investigation of the intramolecular motions undergone by transition metal complexes of chalcogen-containing ligands [1,2], we have recently studied metal complexes formed by ligands in which a metallocene fragment forms the backbone of the ligand. In this context we have reported on complexes formed by the ligands 1,1′-bis(methylthio)ferrocene (BMSF) and 1,1′-bis(methylseleno)ferrocene (BMSEF), with the Group VI carbonyls [3], the organoplatinum(IV) halides, $[(PtXMe_3)_4]$ (X = Cl, Br, I) [4] and the carbonyl halides of rhenium $[ReX(CO)_5]$ (X = Cl, Br, I) [5]. We have now extended these studies to include a ligand derived from ruthenocene, namely 1,1′-bis(methylthio)-ruthenocene (BMSR).

Here we report the synthesis and spectroscopic properties of the complexes *cis*-$[M(CO)_4(BMSR)]$ (M = Cr, Mo, W), *fac*-$[ReX(CO)_3(BMSR)]$ (X = Cl, Br, I), *fac*-$[PtXMe_3(BMSR)]$ (X = Cl, Br, I), the sulphur inversion energy, and the crystal and molecular structure of *cis*-$[W(CO)_4(BMSR)]$. The main aim of this study was to compare the structures of these ruthenocenophane molecules in solution and the energies of their fluxional processes with those of analogous ferrocenophane molecules.

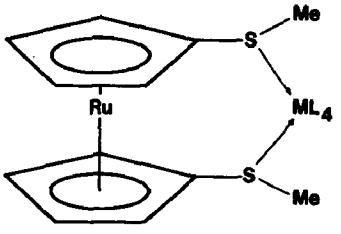

	ML_4
I	$Cr(CO)_4$
II	$Mo(CO)_4$
III	$W(CO)_4$
IV	$PtClMe_3$
V	$PtBrMe_3$
VI	$PtIMe_3$
VII	$ReCl(CO)_3$
VIII	$ReBr(CO)_3$
IX	$ReI(CO)_3$

Experimental

General

All preparations were carried out by standard Schlenk techniques [6]. All reactions were performed under purified nitrogen in freshly distilled, dried and degassed solvents.

The following compounds were prepared by published methods; *cis*-$[M(CO)_4(nbd)]$ (M = Cr, Mo) [7], (nbd = bicyclo[2.2.1]hepta-2,5-diene) (M = W) [8], *fac*-$[M(CO)_3(NCCH_3)_3]$ (M = W) [9], $[ReX(CO)_5]$ (X = Cl, Br, I) [10,11], $[(PtXMe_3)_4]$ (X = Cl, Br, I) [12,13,14], $[PtXMe_3(Me_2S)_2]$ (X = Cl, Br, I) [15].

Infrared spectra were recorded on a Perkin Elmer 881 infrared spectrophotometer, calibrated with the 1602 cm^{-1} signal of polystyrene.

Elemental analyses were performed by Butterworth Laboratories Ltd., Teddington, Middlesex, London and by C.H.N. Analysis, South Wigston, Leicester.

Synthesis of ligand

1,1′-Bis(methylthio)ruthenocene (BMSR) was prepared by a route analogous to that used for BMSF and BMSEF [3]. The crude product was subjected to dry-col-

umn chromatography on neutral grade II alumina. A pale yellow band was observed on elution with hexane/benzene (1/1), and after removal of the solvent under reduced pressure this left a pungent-smelling, yellow, viscous oil. Yield 1.42 g, (51%). ^{1}H NMR data ($CDCl_3$ solution): δ 2.29(s), CH_3S; 4.59(t), H(3,4) (ring protons); 4.76(t), H(2,5) (ring protons).

Synthesis of complexes

Each group of complexes was prepared in a similar fashion, the reaction time being the only variable. A typical example from each group is given below, and details of all the synthetic, analytical and infrared data are summarised in Table 1.

(i) Group 6 metal tetracarbonyl complexes. To a solution of $[W(CO)_4(nbd)]$ (0.33 g, 0.85 mmol) in hexane (50 cm^3) was added BMSR (0.30 g, 0.929 mmol). The solution was stirred and refluxed for 55 h, the progress of the reaction being monitored by infrared spectroscopy. A dark green-brown suspension was formed, and this was filtered and the filtrate was evaporated to dryness. The resulting solid was washed with cold hexane (2×10 cm^3), and then recrystallised from hexane/dichloromethane (1/1) to give well-formed pale lemon-yellow crystals of *cis*-$[W(CO)_4(BMSR)]$. Yield, 0.129 g (25%).

(ii) Tricarbonylrhenium(I) halide complexes. To a solution of $[ReCl(CO)_5]$ (0.27 g, 0.75 mmol) in tetrahydrofuran (40 cm^3) was added BMSR (0.28 g, 0.87 mmol), and the mixture stirred and refluxed for 20 h. The resulting pale yellow solution was filtered and evaporated to dryness. The solid was washed with hexane and recrystallised from hexane/dichloromethane (1/1) to give off-white translucent crystals of *fac*-$[ReCl(CO)_3(BMSR)]$. Yield, 0.305 g (65%).

(iii) Trimethylplatinum(IV) halide complexes. To a solution of $[PtClMe_3(Me_2S)_2]$ (0.34 g, 0.85 mmol) in benzene (50 cm^3) was added BMSR (0.30 g, 0.93 mmol) and the mixture was refluxed for 16 h. To aid completion of the reaction, the benzene and the displaced Me_2S were removed under vacuum and replaced by fresh benzene (20 cm^3). Refluxing was continued for a further 6 h, when the light-brown solution was filtered and evaporated to dryness. The off-white solid was washed with hexane (2×20 cm^3) and benzene (2×20 cm^3). The product was sparingly soluble in 1,1,2,2-tetrachloroethane and attempted recrystallisation gave only an off-white powder of *fac*-$[PtClMe_3(BMSR)]$. Yield, 0.215 g (42%).

NMR studies

^{1}H and ^{195}Pt-{^{1}H} NMR spectra were recorded on a Bruker AM250 FT spectrometer, operating at 250.13 and 53.53 MHz, respectively. The spectra were recorded with $CDCl_3$, CD_2Cl_2 or $C_2D_4Cl_4$ solutions. ^{1}H chemical shifts are quoted relative to Me_4Si as internal standard, and the ^{195}Pt chemical shift is quoted relative to $\Xi(^{195}Pt)$ 21.4 MHz.

A standard B-VT1000 variable temperature unit was used to control the probe temperature, with the calibration of this unit being checked periodically against a Comark digital thermometer. The temperatures are considered accurate to $\pm 1°C$. Bandshape analyses were performed with modified versions of the program DNMR of Kleier and Binsch [16,17].

X-ray structure determination

Crystal data for $C_{16}H_{14}O_4RuS_2W$ M 619.32, triclinic, space group $P\bar{1}$, a 7.603(1), b 14.668(2), c 9.054(1) Å, α 106.63(1), β 103.91(1), γ 77.31(1)°, U 926.6(2) Å^3,

$Z = 2$, D_c 2.220 g cm^{-3}, $F(000) = 584$, λ 0.71069 Å, μ (Mo-K_α) 73.7 cm^{-1}, crystal size 0.55 × 0.40 × 0.20 mm.

Data collection. Unit cell parameters and intensity data were obtained by previously detailed procedures [18] on a CAD4 diffractometer using graphite-monochromated Mo-K_α radiation and an ω–2θ scan mode. A total of 3249 unique reflections were collected ($3 \leq 2\theta \leq 50°$). The segment of reciprocal space scanned was: h, −9–9; k, 0–17; l, −10–10. The reflection intensities were corrected for absorption, using the azimuthal-scan method [19]; maximum and minimum transmission factors 1.00, 0.73.

Solution and refinement of structure. The structure was solved by the application of routine heavy-atom methods (SHELX-84) [20], and refined by full-matrix least squares (SHELX-76) [21]. All non-hydrogen atoms were refined anisotropically and hydrogen atoms were not included in the final model. The final residuals R and R_w were 0.025 and 0.028 respectively for the 217 variables and 3068 reflections for which $F_o > 6\sigma(F_o)$. The function minimised was $\Sigma w(|F_o| - |F_c|)^2$, with the weight, w, being defined as $1/[\sigma^2(F_o) + 0.00005\,F_o^2]$. Atomic scattering factors and anomalous scattering parameters were taken from references [22] and [23], respectively. All computations were made on a DEC VAX-11/750 computer. A complete table of bond lengths and angles, and lists of thermal parameters and structure factors are available from the authors.

Results and discussion

The ligand BMSR reacts with $[M(CO)_4(nbd)]$ (M = Cr, Mo, W), $[ReX(CO)_5]$ (X = Cl, Br, I), $[(PtXMe_3)_4]$ (X = Cl, Br, I) to yield the complexes *cis*-$[M(CO)_4(BMSR)]$, *fac*-$[ReX(CO)_3(BMSR)]$ and *fac*-$[PtXMe_3(BMSR)]$, respectively. Data for the preparation and characterisation of the complexes are listed in Table 1. The compounds were isolated as pale yellow or off-white crystalline solids. The Group VI compounds decompose on standing in air, but the Pt and Re compounds are air- and light-stable both in the solid state and in solution. All the compounds are less soluble in organic solvents than the corresponding ferrocene derivatives, the platinum compounds having the lowest solubility.

Group VIA metal tetracarbonyl complexes

NMR spectroscopy. Complexes I, II and III were investigated by variable temperature ^{1}H spectroscopy and the data obtained are listed in Table 2.

Low temperature data for the chromium and molybdenum complexes (I and II) could not be obtained because of separation of the compounds from solution at ca. −100 °C. At this temperature the species were still undergoing exchange broadening and hence the low-temperature limiting spectra could not be obtained. Complex III was studied in some detail. At −90 °C the spectrum indicated the presence of two solution species of very similar populations. In the ring methine region the situation was similar to that observed for 1,1′-bis(methylthio)ferrocene (BMSF) and 1,1′-bis(methylseleno)ferrocene (BMSEF) complexes [3] except that all the signals were of approximately similar intensity. Two sets of ABCD spin systems could be identified. When the temperature of the sample was raised, certain bands within the two sets underwent exchange broadening until two averaged signals consistent with an AA′BB′ spin system were observed at room temperature. These

Table 1

Synthesis and characterisation of the complexes $[ML_4(BMSR)]$ ($ML_4 = Cr(CO)_4$, $Mo(CO)_4$, $W(CO)_4$, $PtXMe_3$, $ReX(CO)_3$)

Complex	Reaction Time (h)	Yield [a] (%)	Melting point (°C)	ν(CO) [b] (cm^{-1})	Analyses (Found (calcd.) (%))	
					C	H
cis-$[Cr(CO)_4(BMSR)]$ (I)	40	35	110–115(dec.)	2017(m) 1900(vs,br) 1856(s)	39.6 (39.4)	2.8 (2.9)
cis-$[Mo(CO)_4(BMSR)]$ (II)	40	23	115–120(dec.)	2026(m) 1913(vs,br) 1858(m)	36.0 (36.2)	2.8 (2.6)
cis-$[W(CO)_4(BMSR)]$ (III)	55	25	173–175	2020(m) 1900(vs,br) 1855(s)	30.5 (31.0)	2.5 (2.3)
fac-$[PtClMe_3(BMSR)]$ (IV)	22	42	215–220(dec.)		30.1 (30.1)	3.7 (3.8)
fac-$[PtBrMe_3(BMSR)]$ (V)	22	34	215–220(dec.)		28.5 (28.0)	2.8 (3.6)
fac-$[PtIMe_3(BMSR)]$ (VI)	22	30	225–230(dec.)		26.0 (26.1)	3.4 (3.3)
fac-$[ReCl(CO)_3(BMSR)]$ (VII)	20	65	206–208	2031(s) 1934(m) 1895(s)	28.8 (28.6)	2.4 (2.2)
fac-$[ReBr(CO)_3(BMSR)]$ (VIII)	20	51	174–176	2033(s) 1936(m) 1899(s)	26.8 (26.8)	2.2 (2.1)
fac-$[ReI(CO)_3(BMSR)]$ (IX)	60	55	210–212(dec.)	2031(s) 1936(m) 1900(s)	25.1 (25.0)	2.0 (1.9)

[a] Yields quoted relative to $[M(CO)_4(nbd)]$, $[PtXMe_3]$ and $[ReX(CO)_5]$, respectively. [b] Recorded in CH_2Cl_2 solution, m, medium; s, strong; vs, very strong; br, broad.

spectral changes may result from pyramidal inversion of the coordinated sulphur atoms and/or reversal of the $SM(CO)_4S$ part of the psuedo six-membered ruthenocenophane ring. If either or both of these processes are slow on the NMR timescale, four invertomers can exist, namely, *meso*-**1**, *meso*-**2**, and a DL degenerate pair. The interrelationship of these species is shown in Fig. 1.

Table 2

^1H NMR parameters for the complexes $[M(CO)_4(BMSR)]$ in CD_2Cl_2 at ambient and low temperatures

Complex		Temperature (°C)	Solution species	Invertomer population (%)	Chemical shift S-Me protons (δ)	Chemical shift ring protons (δ)	
No.	M						
I	Cr	30	*meso*/DL	100	2.64(s)	5.07	4.69 [a]
II	Mo	30	*meso*/DL	100	2.69(s)	5.05(t)	4.71(t)
III	W	30	*meso*/DL	100	2.88(t) [2.4] [c]	5.07(t)	4.74(t)
III	W	−90	DL	48	2.77(s)	4.97 4.64	4.94 [b] 4.65
III	W	−90	*meso*	52	2.81(s)	5.10 4.77	4.90 4.52

[a] Broadened signals due to slight paramagnetism. [b] Signals not resolvable. [c] ^3J(WH) values in Hz, s, singlet; t, triplet.

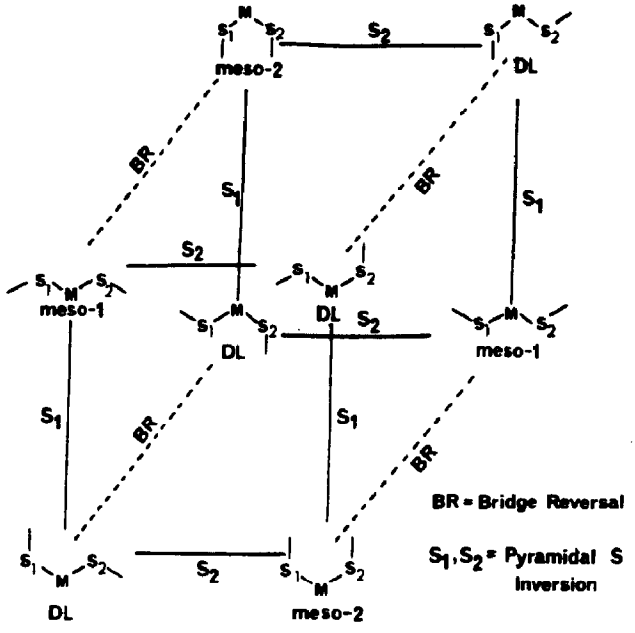

Fig. 1. Graph diagram showing the relationships of the static invertomer species of $[M(CO)_4\{(C_5H_4SCH_3)_2Ru\}]$.

For the reasons outlined in the study of the BMSF and BMSEF complexes [3], rapid bridge reversal can be assumed, and hence there is a rapid interchange between adjacent structures of the front and rear faces of the cube diagram, Fig. 1. It follows that the bandshape changes are entirely due to sulphur inversion interchanging bridge reversal-averaged *meso* and DL species. The degenerate DL pairs will thus be observed as psuedo-planar –S–M–S– bridge structures, whilst the *meso*-**1** structure will be highly favoured over *meso*-**2** owing to the steric interaction of the *S*-methyls, both with each other and with adjacent ring protons in the latter invertomer. Sulphur inversion thus leads to an exchange of species as shown.

$$\langle \textit{meso}\text{-}\mathbf{1}/\textit{meso}\text{-}\mathbf{2}\rangle \rightleftharpoons \langle \mathrm{DL}/\mathrm{DL}\rangle$$

$$\approx \textit{meso}\text{-}\mathbf{1} \qquad\qquad \Vert \uparrow$$

$$\Vert \uparrow$$

$$\langle \mathrm{DL}/\mathrm{DL}\rangle \rightleftharpoons \langle \textit{meso}\text{-}\mathbf{2}/\textit{meso}\text{-}\mathbf{1}\rangle$$

$$\approx \textit{meso}\text{-}\mathbf{1}$$

The two sets of signals in the low-temperature spectrum can be attributed to these two conformationally-averaged species. The relative populations of the invertomers were found to be 52/48; *meso*/DL. The *meso* structure is suggested to be the more populous for several reasons. Firstly in the analogous BMSF and BMSEF complexes, the *meso* invertomer signals in the *E*-methyl region always lie to higher frequency of the DL signals. For complex III the signal at δ 2.81 is of higher intensity than the signal at δ 2.77. Secondly, in the ring-methine region, the *meso* configuration always gives rise to a signal at considerably higher frequency than any of the others. This is also the pattern for III for the more intense set of signals.

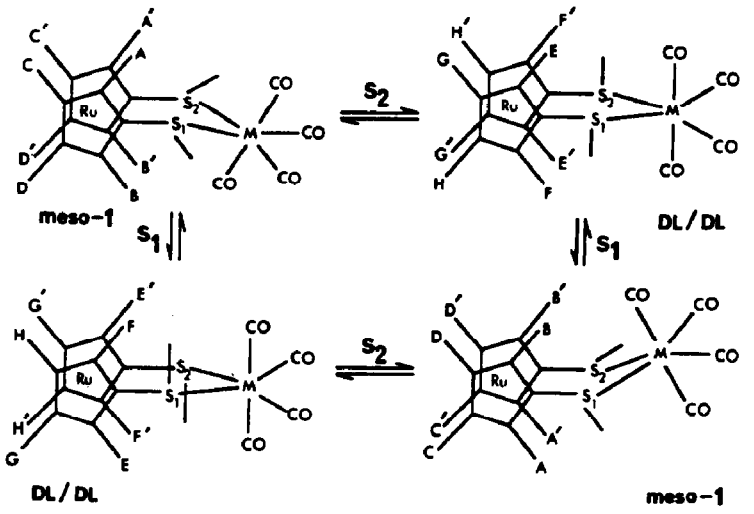

Fig. 2. The bridge reversal-averaged invertomers of complex III showing the methine proton labelling.

Finally in the crystal structure of III (see later) the *meso* configuration of the *S*-methyls is adopted.

Although it was only possible to study the tungsten complex in detail, it is interesting to note the effect of the ruthenocenyl backbone on the relative population of invertomers. For the BMSF and BMSEF complexes the DL invertomer was greatly favoured over the *meso* structure [3]. With the increased inter-ring distance of the ruthenocenyl moiety compared with the ferrocenyl species (3.68 Å [24] versus 3.32 Å [25]) the *meso* structure is now slightly more favoured. This change is presumably associated with a reduction in the steric hindrance of the *S*-methyls and ring protons in the *meso* structure.

Dynamic NMR studies. The energetics of pyramidal sulphur inversion were then investigated for complex III by using the ring-methine protons as the structural probes. The labelling scheme is as shown in Fig. 2. Each solution species consists of an 8-spin system, but by following the procedure adopted in the study of the BMSF complexes [3], this can be simplified to two sub-systems of single spins exchanging between four different chemical configurations, i.e:

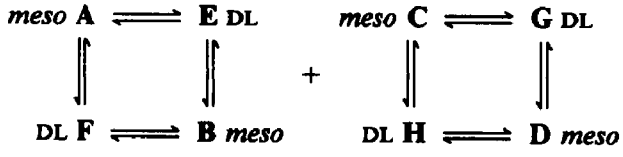

Identification of the two sets of four exchanging signals was achieved by observation of the exchanges in the variable-temperature spectra, from which it was clear that the four higher frequency ring-methine signals exchange and coalesce together as do the four lower frequency signals (Fig. 3). Thus there is a distinct separation and no overlap of the two sets of exchanging signals. Precise assignment of some of the signals within the sets was not possible, but the correct separation of the eight signals into the two exchanging sets essential for bandshape analysis was confirmed by the excellent fits obtained between experimental and theoretical

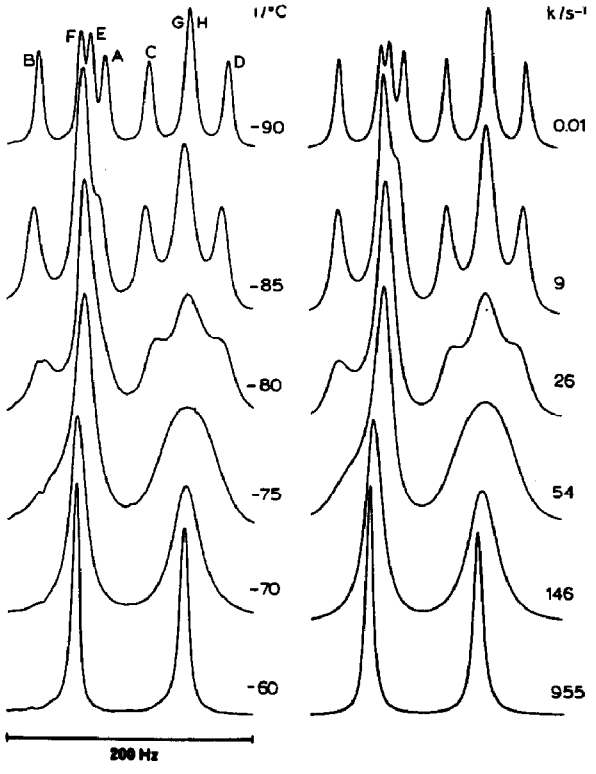

Fig. 3. The experimental (left) and computer synthesised ^{1}H NMR spectra (methine region) of [W(CO)$_4$(BMSR)] showing the 'best fit' rate constants for each temperature.

spectra (Fig. 3). The analysis was performed in the temperature range -90 to $-60\,^\circ$C and the activation parameters obtained are listed in Table 3.

The ΔG^* (298 K) value found for III is identical within experimental error to that found for the analogous complex [W(CO)$_4$(BMSF)], namely 32.0 ± 1.0 and 31.5 ± 0.6 kJ mol^{-1} respectively. Thus it appears that the introduction of the ruthenocenyl fragment into the complex does not significantly affect the sulphur inversion barrier. Features that affect sulphur inversion, such as strengths of bonds and electron density around the inverting atom do not appear to be changed by the ruthenocenyl group, possibly because of its relative remoteness from the inverting sulphur atoms. Large values of $\log_{10}A$ and ΔS^* are again observed [3,4,5], which are interpreted as indicating the presence of a rapid ring conformational process.

X-ray crystallography

Atomic parameters for the crystal structure of [W(CO)$_4$(BMSR)] are given in Table 4. A view of the molecule drawn with the program ORTEP [26] and showing

Table 3

Arrhenius and Eyring activation parameters for pyramidal sulphur inversion (*meso* → DL) in complex III

Complex	E_a (kJ mol^{-1})	$\log_{10}A$	ΔH^* (kJ mol^{-1})	ΔS^* (J K^{-1} mol^{-1})	ΔG^* (298 K) (kJ mol^{-1})
III	60.7±2.0	17.8±0.5	59.0±2.0	90.7±9.9	32.0±1.0

Table 4

Fractional atomic coordinates [a] ($\times 10^4$) for $[W(CO)_4(BMSR)]$

	x	y	z
W	951.8(3)	2646.0(2)	1460.1(3)
Ru	−2571.9(6)	2215.5(3)	−3154.3(5)
S(1)	−952(2)	3941(1)	56(2)
S(2)	1826(2)	1884(1)	−1245(2)
O(1)	−2192(8)	1478(5)	1210(7)
O(2)	3547(7)	1093(4)	3055(8)
O(3)	74(8)	3784(4)	4764(6)
O(4)	4318(8)	3760(5)	2290(7)
C(1)	−1113(9)	1903(5)	1205(8)
C(2)	2576(9)	1689(5)	2449(8)
C(3)	393(9)	3359(5)	3497(8)
C(4)	3077(9)	3367(5)	1929(7)
C(5)	−2167(10)	4905(5)	1389(9)
C(6)	3621(9)	836(5)	−1199(10)
C(7)	−2811(7)	3580(4)	−1439(7)
C(8)	−3132(9)	3757(4)	−2968(8)
C(9)	−4724(9)	3360(5)	−3869(9)
C(10)	−5380(8)	2915(5)	−2902(9)
C(11)	−4182(8)	3063(4)	−1372(8)
C(12)	88(7)	1395(4)	−2759(7)
C(13)	−265(8)	1537(4)	−4308(7)
C(14)	−1832(8)	1080(5)	−5170(8)
C(15)	−2389(8)	652(4)	−4189(8)
C(16)	−1201(8)	834(4)	−2670(8)

[a] Esd's, given in parentheses, are applicable to the least significant digits.

the numbering scheme adopted is shown in Fig. 4. This displays the expected *cis* octahedral coordination for W, the chelating nature of the ligand, and the *meso* relationship of the S-CH_3 groups. Bond distances and selected bond angles are given in Tables 5 and 6, respectively.

The ruthenium to carbon distances range from 2.156(8) to 2.202(8) Å and are comparable to values reported for other ruthenocene derivatives [27,28]. The carbon–carbon distances in the cyclopentadienyl rings vary from 1.408(10) to 1.457(10) Å and the C–C–C bond angles within the two rings vary from 106.5 to 109.6°. Differences in the exocyclic C–C–S bond angles, means 122.8 and 127.8°, are also observed. This is a structural feature which is common to sulphur and selenium ferrocenophanes and ruthenocenophanes of this type [29]. The W–S bond lengths are 2.571(5) and 2.565(4) Å, values comparable to those found in other compounds which contain tungsten(0) bonded to sulphur [30,31].

Inspection of the bond angles at W (Table 6) shows that there is considerable distortion from a regular octahedral structure at W, the principal deviations involving the angles S–W–S, at 81.8(1)°, C(1)–W–S(1), at 97.1(3)° and C(1)–W–S(2), at 98.4(3)°, compared with the ideal value of 90°. The W–C distances *trans* to S at 1.930(9) and 1.937(9) Å are shorter than the corresponding distances *cis* to S at 2.035(9) and 2.018(9) Å. This effect has been observed in other metal–sulphur bonded derivatives of the Group VI carbonyls, [31,32] and has been attributed to competition of the *trans* carbonyl ligands for the electron density from the W atom.

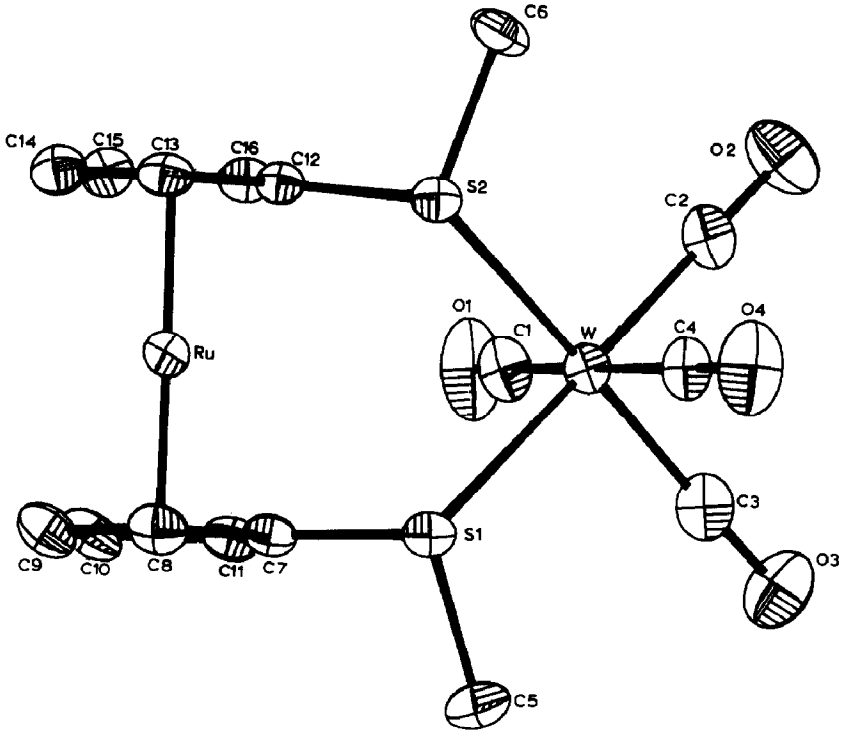

Fig. 4. A view of the X-ray crystal structure of $[W(CO)_4(BMSR)]$.

In the crystal studied the S–CH_3 groups adopt a *meso* relationship, although in solution at low temperatures, as indicated by NMR measurements, the *meso* and DL conformers are found to be of approximately equal abundance (Table 2).

Table 5

Bond lengths (Å) [a] for $[W(CO)_4(BMSR)]$

S(1)–W	2.571(5)	S(2)–W	2.565(4)
C(1)–W	2.035(9)	C(2)–W	1.930(9)
C(3)–W	1.937(9)	C(4)–W	2.018(8)
C(7)–Ru	2.156(8)	C(8)–Ru	2.172(8)
C(9)–Ru	2.196(8)	C(10)–Ru	2.191(8)
C(11)–Ru	2.186(8)	C(12)–Ru	2.120(7)
C(13)–Ru	2.163(7)	C(14)–Ru	2.182(8)
C(15)–Ru	2.202(8)	C(16)–Ru	2.178(8)
C(5)–S(1)	1.815(8)	C(7)–S(1)	1.763(8)
C(6)–S(2)	1.820(8)	C(12)–S(2)	1.767(8)
C(1)–O(1)	1.135(8)	C(2)–O(2)	1.187(9)
C(3)–O(3)	1.192(9)	C(4)–O(4)	1.145(9)
C(8)–C(7)	1.435(10)	C(11)–C(7)	1.438(9)
C(9)–C(8)	1.426(10)	C(10)–C(9)	1.457(10)
C(11)–C(10)	1.450(10)	C(13)–C(12)	1.430(9)
C(16)–C(12)	1.440(9)	C(14)–C(13)	1.442(10)
C(15)–C(14)	1.408(10)	C(16)–C(15)	1.442(10)

[a] Esd's, given in parentheses, are applicable to the least significant digits.

Table 6

Selected bond angles (°) [a] for $[W(CO)_4(BMSR)]$ (III)

S(1)–W–S(2)	81.8(1)		
C(1)–W–S(1)	97.1(3)	C(1)–W–S(2)	98.4(3)
C(2)–W–S(1)	174.7(2)	C(2)–W–S(2)	94.9(3)
C(3)–W–S(1)	94.2(3)	C(3)–W–S(2)	173.1(2)
C(4)–W–S(1)	87.1(3)	C(4)–W–S(2)	85.9(3)
C(3)–W–C(1)	87.7(4)	C(4)–W–C(1)	174.4(2)
C(3)–W–C(2)	88.6(4)	C(4)–W–C(2)	88.4(4)
C(4)–W–C(3)	88.3(4)	C(2)–W–C(1)	87.6(4)
O(2)–C(2)–W	178.8(6)	O(1)–C(1)–W	173.2(6)
O(4)–C(4)–W	175.4(6)	O(3)–C(3)–W	178.7(7)
C(5)–S(1)–W	110.7(4)	C(6)–S(2)–W	111.3(4)
C(7)–S(1)–W	115.9(3)	C(12)–S(2)–W	116.2(3)
C(8)–C(7)–S(1)	122.8(6)	C(13)–C(12)–S(2)	122.8(6)
C(11)–C(7)–S(1)	127.6(6)	C(16)–C(12)–S(2)	127.9(6)
C(11)–C(7)–C(8)	109.6(6)	C(16)–C(12)–C(13)	109.2(6)
C(9)–C(8)–C(7)	107.5(7)	C(14)–C(13)–C(12)	106.5(6)
C(10)–C(9)–C(8)	108.4(7)	C(15)–C(14)–C(13)	109.1(7)
C(11)–C(10)–C(9)	107.7(7)	C(16)–C(15)–C(14)	108.6(7)
C(10)–C(11)–C(7)	106.8(7)	C(15)–C(16)–C(12)	106.5(7)

[a] Esd's, given in parentheses, are applicable to the least significant digits.

Figure 4 shows that the cyclopentadienyl rings are, within the limits of error, planar and also parallel. The dihedral angle between the rings is very small, as was also the case in the $[W(CO)_4(BMSEF)]$ and $[ReCl(CO)_3(BMSF)]$ complexes. There is some displacement of the S atoms from the planes of the rings to which they are attached, towards the Ru atom, giving a non-bonded S–S separation of 3.364 Å compared with the C(7)–C(12) distance of 3.538 Å

Tricarbonylrhenium (I) halide complexes

Ambient and low-temperature ^1H spectra were recorded for the complexes VII, VIII, and IX. The chemical shift and invertomer population data are given in Table 7. The invertomer populations were deduced from the number of signals in the ring methine and S–methyl regions of the spectrum. For VIII and IX the single S–methyl signal and the four strong signals of equal intensity in the ring-methine region indicate the presence of only a *meso* form at low temperatures, whereas for VII, the appearance of two weak S–methyl signals at δ 2.95 and 2.67, suggests the presence of a trace of a DL invertomer.

As found for the Group 6A metal BMSR complexes, the invertomer populations are greatly changed compared with those for the analogous BMSF and BMSEF complexes [5]. For VII, VIII and IX a *meso* invertomer is overwhelmingly favoured over the DL structures, and the halogen dependence of invertomer populations which is usually observed in $ReX(CO)_3$ species [33,34,35] appears to have been completely lost. It appears that the increased inter-ring distance of the metallocenyl fragment results in a *meso* structure, presumably *meso*-**1**, which is greatly favoured over the DL forms. The massive predominance of a single *meso* invertomer precluded investigation of the dynamic behaviour of these complexes.

Table 7

^{1}H NMR shifts for the complexes [ReX(CO)$_3$(BMSR)] in CD_2Cl_2 solution at ambient and low temperatures

Complex No.	X	Temperature (°C)	Solution species	Invertomer population (%)	Chemical shift S-Me protons (δ)	Chemical shift ring protons (δ) [a]
VII	Cl	30	*meso*/DL	100	2.93	5.26 5.19 4.89 4.71
VII	Cl	−80	*meso*	94	2.91	5.25 4.87 5.13 4.65
VII	Cl	−80	DL	6	2.95 2.67	[b]
VIII	Br	30	*meso*/DL	100	2.95	5.28 5.18 4.90 4.70
VIII	Br	−80	*meso*	[c]	2.92	5.22 4.84 5.12 4.63
VIII	Br	−80	DL	[c]	2.74 [b]	[b]
IX	I	30	*meso*/DL	100	2.98	5.28 4.93 5.17 4.70
IX	I	−80	*meso*	~100	2.92	5.21 4.85 5.12 4.62
IX	I	−80	DL	~0	[b]	[b]

[a] Signals show weak multiplet structure in most cases. [b] DL signals not observed due to low intensity and overlap. [c] Populations not determined due to overlap of *meso* and DL species.

Trimethylplatinum(IV) halide complexes

Investigations of the structures and possible dynamic behaviour of complexes IV, V and VI were severely curtailed by the insolubility of the materials. They were sparingly soluble in deutero-1,1,2,2-tetrachloroethane, but only ambient temperature ^{1}H spectra could be recorded, when any spectral changes attributable to pyramidal sulphur inversion are complete and signals arise from averaged *meso*/DL interconverted species. The ^{1}H spectral parameters are listed in Table 8. The coupling constants show a good correlation with those found for analogous BMSF complexes [4], as do the chemical shifts, except in the ring-methine region where the signals are shifted downfield by ~ 0.3–0.4 ppm.

Table 8

^{1}H NMR data for the complexes [PtXMe$_3$(BMSR)] in $(CDCl_2)_2$

Complex No.	X	Temperature (°C)	Invertomer	Chemical shift Pt-Me protons (δ)	Chemical shift S-Me protons (δ)	Chemical shift ring protons (δ) [a]
IV	Cl	30	*meso*/DL	1.17(t) [71.7] [b] 1.11(t) [71.1] [b]	2.58(t) [13.2] [c]	5.42 4.88 4.74
V	Br	30	*meso*/DL	1.26(t) [71.6] [b] 1.21(t) [70.4] [b]	2.62(t) [13.8] [c]	5.45 4.90 4.71
VI	I	30	*meso*/DL	1.38(t) [72.4] [b] 1.35(t) [71.9] [b]	2.67(t) [13.9] [c]	5.50 4.89 4.71

[a] Signals show weak multiplet structure in most cases. [b] ^2J(PtH) values in Hz. [c] ^3J(PtH) values in Hz; t, triplet.

A proton-decoupled ^{195}Pt spectrum of IV at $-50\,^{\circ}C$ in $(CDCl_2)_2$ was recorded and a single chemical shift δ 2465 (relative to $\Xi(^{195}Pt)$ 21.4 MHz) was observed. In the case of $PtXMe_3$-BMSF and -BMSEF complexes the DL invertomer is always preferred to the *meso*, by not less than 90/10, but with BMSR complexes the invertomer populations are expected to be more evenly balanced. Nevertheless the DL invertomer is likely to be the dominant species and hence the ^{195}Pt signal is attributed to this species. The value of δ 2465 can be compared with that of 1597 for the DL invertomer of the very similar complex $[PtClMe_3(BMSF)]$ [4]. The high frequency shift of 868 ppm is not unusual in ^{195}Pt spectra, in which the chemical shifts are known to be extremely sensitive to electronic and steric effects and to cover an extremely wide range of values [36,37]. In the case of IV it is clearly the replacement of iron by ruthenium in the backbone that has produced the change in chemical shift.

In conclusion it is obvious that in so far as we were able to perform detailed measurements on the BMSR complexes, the sulphur inversion energy was found to be virtually unaffected by a change from a ferrocenyl to a ruthenocenyl backbone for the ligand, but in contrast the relative proportions of the invertomers are strongly influenced.

Acknowledgement

We thank the University of Exeter for the award of a Frank Southerden Scholarship to N.J.L.

References

1 E.W. Abel, S.K. Bhargava, and K.G. Orrell, Prog. Inorg. Chem., 32 (1984) 1.
2 K.G. Orrell and V. Šik, Ann. Rep. NMR Spectrosc., 19 (1987) 79.
3 E.W. Abel, N.J. Long, K.G. Orrell, A.G. Osborne, V. Šik, P.A. Bates, and M.B. Hursthouse, J. Organomet. Chem., 367 (1989) 275.
4 E.W. Abel, N.J. Long, K.G. Orrell, A.G. Osborne and V. Šik, J. Organomet. Chem., 378 (1989) 473.
5 E.W. Abel, N.J. Long, K.G. Orrell, A.G. Osborne, V. Šik, P.A. Bates and M.B. Hursthouse, J. Organomet. Chem., 383 (1990) 253.
6 D.F. Shriver, Manipulation of Air-Sensitive Compounds, McGraw-Hill, New York, 1969.
7 M.A. Bennett, L.A. Pratt and G. Wilkinson, J. Chem. Soc., (1961) 2037.
8 R.B. King and A. Fronzaglia, Inorg. Chem., 5 (1966) 1837.
9 D.P. Tate, J.M. Augl and W.R. Knipple, Inorg. Chem., 1 (1962) 433.
10 W. Hieber, R. Schuh and H. Fuchs, Z. Anorg. Allg. Chem., 248 (1941) 243.
11 M.M. Bhatti, Ph.D. Thesis, University of Exeter, 1980.
12 J.C. Baldwin and W.C. Kaska, Inorg. Chem., 14 (1975) 2020.
13 D.E. Clegg and J.R. Hall, Spectrochim. Acta, 21 (1965) 357.
14 D.E. Clegg and J.R. Hall, J. Organomet. Chem., 22 (1970) 491.
15 E.W. Abel, A.R. Khan, K. Kite, K.G. Orrell and V. Šik, J. Organomet. Chem., 225 (1982) 357.
16 D.A. Kleier and G. Binsch, J. Magn. Reson., 3 (1970) 146.
17 D.A. Kleier and G. Binsch, DNMR 3 Program 165, Quantum Chemistry Program Exchange, Indiana University, 1970.
18 M.B. Hursthouse, R.A. Jones, K.M.A. Malik and G. Wilkinson, J. Am. Chem. Soc., 101 (1979) 4128.
19 A.C.T. North, D.C. Phillips and F.S. Mathews, Acta Crystallogr., A, 24 (1968) 351.
20 G.M. Sheldrick, SHELX-84 Program for Crystal Structure Solution, private communication.
21 G.M. Sheldrick, SHELX-76 Program for Crystal Structure Determination and Refinement, University of Cambridge, 1976.
22 D.T. Cromer and J.B. Mann, Acta. Crystallogr., A, 24 (1968) 321.

23 D.T. Cromer and D. Liberman, J. Chem. Phys., 53 (1970) 1891.
24 G.L. Hardgrove and D.H. Templeton, Acta Crystallogr., 12 (1959) 28.
25 J.D. Dunitz, L.E. Orgel and A. Rich, Acta Crystallogr., 9 (1956) 373.
26 C.K. Johnson, ORTEP II, A Fortran Thermal Ellipsoid Plotting Program Crystal Structure Illustrations, ORNL Report 3794. Oak Ridge National Laboratory, Oak Ridge, Tennessee, USA.
27 P. Seiler and J.D. Dunitz, Acta Crystallogr. B, 36 (1980) 2946.
28 S. Ohba, Y. Saito, S. Kamiyama and A. Kasahara, Acta Crystallogr. C, 40 (1984) 53.
29 A.G. Osborne, R.E. Hollands, R.F. Bryan and S. Lockhart, J. Organomet. Chem., 288 (1985) 207.
30 B.K. Balbach, A.R. Koray, A. Okur, P. Wulknitz and M.L. Ziegler, J. Organomet. Chem., 212 (1981) 77.
31 G.H. Barnett, M.K. Cooper, M. McPartlin and G.B. Robertson, J. Chem. Soc. Dalton Trans., (1978) 587.
32 C. Glidewell, D.C. Liles and P.J. Pogorzelec, Acta Crystallogr. C, 39 (1983) 542.
33 E.W. Abel, M.Z.A. Chowdhury, K.G. Orrell and V. Šik, Polyhedron, 3 (1984) 331.
34 E.W. Abel, S.K. Bhargava, M.M. Bhatti, K. Kite, M.A. Mazid, K.G. Orrell, V. Šik, B.L. Williams, M.B. Hursthouse and K.M.A. Malik, J. Chem. Soc. Dalton Trans., (1982) 2065.
35 E.W. Abel, R. Corben, I. Moss, K.G. Orrell, N.R. Richardson and V. Šik, J. Organomet. Chem., 344 (1988) 343.
36 P.S. Pregosin, Ann. Rep. NMR Spectrosc., 17 (1986) 285.
37 K.G. Orrell, Coord. Chem. Rev., 96 (1989) 1.